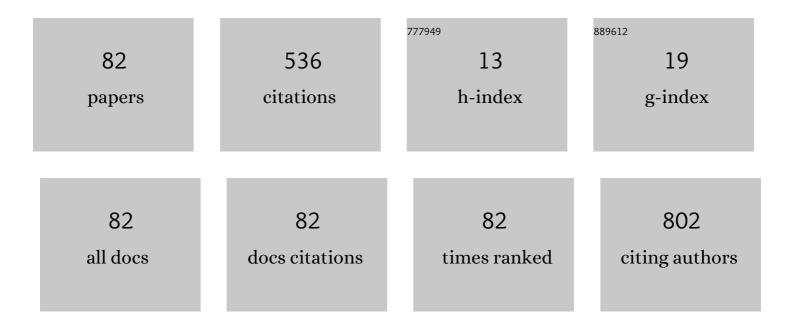
List of Publications by Year in descending order

Source: https://exaly.com/author-pdf/5115316/publications.pdf Version: 2024-02-01



LOFI MOLINA

#	Article	IF	CITATIONS
1	Electrostatically charged rutile TiO2 surfaces with enhanced photocatalytic activity for bacteria inactivation. Catalysis Today, 2022, 392-393, 154-166.	2.2	7
2	Effect of controlled humidity on resistive switching of multilayer VO2 devices. Materials Science and Engineering B: Solid-State Materials for Advanced Technology, 2021, 264, 114968.	1.7	14
3	Influence of selected reactive oxygen species on the photocatalytic activity of TiO2/SiO2 composite coatings processed at low temperature. Applied Catalysis B: Environmental, 2021, 291, 119685.	10.8	27
4	Influence of Laser Modulation Frequency on the Performance of Terahertz Photoconductive Switches on Semi-Insulating GaAs Exhibiting Negative Differential Conductance. IEEE Transactions on Terahertz Science and Technology, 2021, 11, 591-597.	2.0	1
5	Study on the photocatalytic activity of titanium dioxide nanostructures: Nanoparticles, nanotubes and ultra-thin films. Catalysis Today, 2020, 341, 2-12.	2.2	35
6	MIM capacitors as simple test vehicles for the DC/AC characterization of ALD-Al2O3 with auto-correction of parasitic inductance. Microelectronics Reliability, 2020, 104, 113516.	0.9	1
7	Analytical Drain Current Model for a-SiGe:H Thin Film Transistors Considering Density of States. Electronics (Switzerland), 2020, 9, 1016.	1.8	2
8	NiSi2 as a bottom electrode for enhanced endurance of ferroelectric Y-doped HfO2 thin films. Japanese Journal of Applied Physics, 2020, 59, SGGB06.	0.8	2
9	Enhanced photocatalytic bacterial inactivation of atomic-layer deposited anatase-TiO2 thin films on rutile-TiO2 nanotubes. Photochemical and Photobiological Sciences, 2020, 19, 399-405.	1.6	6
10	Spatio-Temporal Defect Generation Process in Irradiated HfO ₂ MOS Stacks: Correlated Versus Uncorrelated Mechanisms. , 2019, , .		1
11	Design and Electrochemical Characterization of Ion-Sensitive Capacitors With ALD Al ₂ O ₃ as the Sensitive Dielectric. IEEE Sensors Journal, 2018, 18, 231-236.	2.4	12
12	Parameter extraction of gate tunneling current in metal–insulator–semiconductor capacitors based on ultra-thin atomic-layer deposited Al2O3. Journal of Materials Science: Materials in Electronics, 2018, 29, 15496-15501.	1.1	6
13	Physical and electrical characterization of yttrium-stabilized zirconia (YSZ) thin films deposited by sputtering and atomic-layer deposition. Journal of Materials Science: Materials in Electronics, 2018, 29, 15349-15357.	1.1	14
14	Room temperature resonant tunneling in metal-insulator-insulator-insulator-semiconductor devices. , 2018, , .		0
15	Resonant tunneling MIIIS diode based on intrinsic quantum-well formation of ultra-thin atomic layered films after band-offset engineering. Applied Surface Science, 2018, 458, 166-171.	3.1	1
16	Rectifying Characteristics of Resonant Tunneling MIS Devices Using Ultra-Thin High-k Oxides Deposited by ALD. IEEE Electron Device Letters, 2018, 39, 1461-1464.	2.2	2
17	Gate modeling of metal–insulator–semiconductor devices based on ultra-thin atomic-layer deposited TiO2. Journal of Materials Science: Materials in Electronics, 2018, 29, 15761-15769.	1.1	5
18	Influence of SiH4 and pressure on PECVD preparation of silicon films with subwavelength structures. Journal of Vacuum Science and Technology B:Nanotechnology and Microelectronics, 2017, 35, .	0.6	2

#	Article	IF	CITATIONS
19	Fundamental study of TiO <inf>2</inf> nanoparticles as photoactive elements for water decontamination. , 2017, , .		0
20	Resistive switching characteristics of MIM structures based on oxygen-variable ultra-thin HfO 2 and fabricated at low temperature. Materials Science in Semiconductor Processing, 2017, 66, 191-199.	1.9	9
21	Accurate modeling of gate tunneling currents in Metal-Insulator-Semiconductor capacitors based on ultra-thin atomic-layer deposited Al2O3 and post-metallization annealing. Thin Solid Films, 2017, 638, 48-56.	0.8	19
22	Localized characterization of charge transport and random telegraph noise at the nanoscale in HfO2 films combining scanning tunneling microscopy and multi-scale simulations. Journal of Applied Physics, 2017, 122, 024301.	1.1	11
23	Understanding the Resistive Switching Phenomena of Stacked Al/Al ₂ O ₃ /Al Thin Films from the Dynamics of Conductive Filaments. Complexity, 2017, 2017, 1-10.	0.9	19
24	Performance of ultraâ€thin HfO ₂ â€based MIM devices after oxygen modulation and postâ€metallization annealing in N ₂ . Physica Status Solidi (A) Applications and Materials Science, 2016, 213, 1807-1813.	0.8	3
25	Single vacancy defect spectroscopy on HfO2 using random telegraph noise signals from scanning tunneling microscopy. Journal of Applied Physics, 2016, 119, .	1.1	20
26	Modeling a mim capacitor including series resistance and inductance for characterizing nanometer highâ€ <i>K</i> dielectric films. Microwave and Optical Technology Letters, 2016, 58, 2599-2602.	0.9	2
27	CAFM based spectroscopy of stress-induced defects in HfO <inf>2</inf> with experimental evidence of the clustering model and metastable vacancy defect state. , 2016, , .		10
28	Analysis of quantum conductance, read disturb and switching statistics in HfO2 RRAM using conductive AFM. Microelectronics Reliability, 2016, 64, 172-178.	0.9	17
29	Conductance-to-Current-Ratio-Based Parameter Extraction in MOS Leakage Current Models. IEEE Transactions on Electron Devices, 2016, 63, 3844-3850.	1.6	12
30	Hermetic capacitive pressure sensors for biomedical applications. Microelectronics International, 2016, 33, 79-86.	0.4	3
31	pH ISFET sensor with PVTA compensation. Electronics Letters, 2016, 52, 15-17.	0.5	2
32	A Generic MEMS Fabrication Process Based on a Thermal Budget Approach. Journal of Electronics Cooling and Thermal Control, 2016, 06, 97-107.	0.4	0
33	Impact of post-deposition annealing on the resistive switching characteristics and forming voltage step of Al/HfO <inf>2</inf> /W structures. , 2015, , .		Ο
34	Role of oxygen vacancies on the resistive switching characteristics of MIM structures fabricated a low temperature. , 2015, , .		0
35	Electrochemical Characterization of Ion-Sensitive Capacitors with ALD Al2O3 as the Sensitive Dielectric. ECS Transactions, 2014, 64, 239-243.	0.3	1
36	Physical and electrical characterization of TiO2 particles after high temperature processing and before and after ultraviolet irradiation. Canadian Journal of Physics, 2014, 92, 832-837.	0.4	2

#	Article	IF	CITATIONS
37	Reduction in the interface-states density of metal-oxide-semiconductor field-effect transistors fabricated on high-index Si (114) surfaces by using an external magnetic field. Journal of Applied Physics, 2014, 116, 064510.	1.1	0
38	Complex Permittivity Determination of Thin-Films Through RF-Measurements of a MIM Capacitor. IEEE Microwave and Wireless Components Letters, 2014, 24, 805-807.	2.0	7
39	Effects of germane flow rate in electrical properties of a-SiGe:H films for ambipolar thin-film transistors. Thin Solid Films, 2014, 562, 260-263.	0.8	6
40	Low-temperature processing of thin films based on rutile TiO2 nanoparticles for UV photocatalysis and bacteria inactivation. Journal of Materials Science, 2014, 49, 786-793.	1.7	15
41	Study of the Chemical and Morphological Characteristics of Al2O3 and HfO2 Surfaces after Immersion in Time-Dependent pH Solutions. ECS Transactions, 2014, 64, 3-9.	0.3	3
42	Influence of the surface roughness of the bottom electrode on the resistive-switching characteristics of Al/Al2O3/Al and Al/Al2O3/W structures fabricated on glass at 300 ŰC. Microelectronics Reliability, 2014, 54, 2747-2753.	0.9	23
43	Planarized ambipolar a-SiGe:H thin-film transistors: Influence of the sequence of fabrication process. Solid-State Electronics, 2014, 99, 45-50.	0.8	9
44	Mechanical characterization of polysilicon cantilevers using a thermo-mechanical test chip fabricated with a combined bulk/surface micromachining technique. Results in Physics, 2014, 4, 119-120.	2.0	4
45	Bulk/surface micromachined polymems test chip for the characterization of electrical, mechanical and thermal properties. , 2014, , .		0
46	Non-homogeneous space mechanical strain induces asymmetrical magneto-tunneling conductance in MOSFETs. , 2014, , .		2
47	Physical and electrical characteristics of atomic-layer deposition-HfO2 films deposited on Si substrates having different silanol Si-OH densities. Journal of Vacuum Science and Technology A: Vacuum, Surfaces and Films, 2013, 31, .	0.9	6
48	Evaluation of interface-states density for MOSFETs fabricated on high-index (114) silicon surfaces. , 2013, , .		0
49	Offset and gain calibration circuit for MIM-ISFET devices. Analog Integrated Circuits and Signal Processing, 2013, 76, 321-333.	0.9	6
50	Using Thin Films of Rutile-Phase TiO2 Nanoparticles as Photoactive Material in Metal-Semiconductor Structures with Low Thermal Processing. Energy and Environment Focus, 2013, 2, 299-306.	0.3	1
51	Atomistic magnetoconductance effects in strained FETs. , 2013, , .		0
52	Chemical and Morphological Characteristics of ALD Al ₂ O ₃ Thin-Film Surfaces after Immersion in pH Buffer Solutions. Journal of the Electrochemical Society, 2013, 160, B201-B206.	1.3	32
53	Performance of a MOHOS-type Memory Using HfO ₂ nanoparticles as Charge Trapping Layer and Ultra-Thin Tunneling Oxide Thickness. Transactions of the Materials Research Society of Japan, 2013, 38, 569-572.	0.2	1
54	Fabrication of Planar Microelectrodes Based on Bulk Silicon Micromachining. IFMBE Proceedings, 2013, , 927-930.	0.2	0

#	Article	IF	CITATIONS
55	Performance of a MOHOS-type memory using np-HfO <inf>2</inf> and variable tunneling oxide thickness. , 2012, , .		0
56	A digitally programmable calibration circuit for smart sensors. , 2012, , .		2
57	Programmable calibration circuit for a MIM-ISFET device. , 2012, , .		0
58	MOHOS-type memory performance using HfO2 nanoparticles as charge trapping layer and low temperature annealing. Materials Science and Engineering B: Solid-State Materials for Advanced Technology, 2012, 177, 1501-1508.	1.7	10
59	MIM-based ISFET sensors with CLOSED/OPEN Sense Plates for pH detection. , 2012, , .		1
60	Integration of MOSFET/MIM Structures Using a CMOS-Based Technology for pH Detection Applications with High-Sensitivity. Procedia Chemistry, 2012, 6, 110-116.	0.7	6
61	HfO2 nanoparticles embedded within a SOG-based oxide matrix as charge trapping layer for SOHOS-type memory applications. Journal of Non-Crystalline Solids, 2012, 358, 2482-2488.	1.5	1
62	Ambipolar a-SiGe:H thin-film transistors fabricated at 200°C. Journal of Non-Crystalline Solids, 2012, 358, 2340-2343.	1.5	9
63	High-quality spin-on glass-based oxide as a matrix for embedding HfO2 nanoparticles for metal-oxide-semiconductor capacitors. Journal of Materials Science, 2012, 47, 2248-2255.	1.7	14
64	Enhancement of the electrical characteristics of MOS capacitors by reducing the organic content of H2O-diluted Spin-On-Glass based oxides. Materials Science and Engineering B: Solid-State Materials for Advanced Technology, 2011, 176, 1353-1358.	1.7	4
65	Spin-On Class as low temperature gate insulator. Materials Research Society Symposia Proceedings, 2011, 1287, 1.	0.1	0
66	Magneto-modulation of gate leakage current in 65nm nMOS transistors: Experimental, modeling, and simulation results. Solid-State Electronics, 2010, 54, 1022-1026.	0.8	3
67	Spin-On Glass as Low-Temperature Gate Insulator for Thin-Film Transistors. , 2010, , .		0
68	Extraction of gate oxide quality and its correlation to the electrical parameters of MOS devices. , 2010, , .		0
69	Progressive-degradation and breakdown of W-La <inf>2</inf> O <inf>3</inf> MOS structures after constant voltage stress. , 2009, , .		0
70	Magnetic field induced gate leakage current in 65nm nMOS transistors. , 2009, , .		1
71	Reliability characteristics of W-La <inf>2</inf> 0 <inf>3</inf> structures compared with those of HfO <inf>2</inf> -based gate oxides. , 2008, , .		0
72	Degradation and Breakdown of W–La2O3Stack after Annealing in N2. Japanese Journal of Applied Physics, 2008, 47, 7076-7080.	0.8	2

#	Article	IF	CITATIONS
73	Effects of N[sub 2]-Based Annealing on the Reliability Characteristics of Tungsten/La[sub 2]O[sub 3]/Silicon Capacitors. Journal of the Electrochemical Society, 2007, 154, G110.	1.3	6
74	Carrier separation and Vth measurements of W-La2O3 gated MOSFET structures after electrical stress. IEICE Electronics Express, 2007, 4, 185-191.	0.3	1
75	Trapping characteristics of lanthanum oxide gate dielectric film explored from temperature dependent current–voltage and capacitance–voltage measurements. Solid-State Electronics, 2007, 51, 475-480.	0.8	39
76	Tunneling in sub-5nm La2O3 films deposited by E-beam evaporation. Journal of Non-Crystalline Solids, 2006, 352, 92-97.	1.5	9
77	Electrical Breakdown and Reliability of Metal Gate - La2O3 Thin Films after Post Deposition Annealing in N2. ECS Transactions, 2006, 1, 757-765.	0.3	1
78	Charge Trapping Characteristics of W-La2O3-nSi MIS Capacitors After Post-Metallization Annealing PMA in N2. ECS Transactions, 2006, 3, 233-244.	0.3	3
79	Degradation of high-K LA2O3 gate dielectrics using progressive electrical stress. Microelectronics Reliability, 2005, 45, 1365-1369.	0.9	21
80	Effects of high-field electrical stress on the conduction properties of ultrathin La2O3 films. Applied Physics Letters, 2005, 86, 232104.	1.5	18
81	Effects of Ambient Temperature on the Electrical Characteristics of Thin La>inf<2>/inf <o>inf<3>/inf<film ,="" .<="" 0,="" by="" e-beam="" evaporation.="" grown="" td=""><td></td><td>1</td></film></o>		1
82	Decoupling the sequence of dielectric breakdown in single device bilayer stacks by radiation-controlled, spatially localized creation of oxide defects. Applied Physics Express, 0, , .	1.1	1